



## 22<sup>nd</sup> IAHR International Symposium on Ice

Singapore, August 11 to 15, 2014

---

# Numerical study on a short-term sea-ice prediction for the Northern Sea Route and Northwest Passage

**Jun Ono**

*National Institute of Polar Research and Graduate School of Frontier Sciences, The University of Tokyo  
Kashiwanoha 5-1-5, Kashiwa, Chiba 277-8561, Japan  
jo@1.k.u-tokyo.ac.jp*

**Liyanarachchi Waruna Arampath De Silva**

*National Institute of Polar Research and Graduate School of Frontier Sciences, The University of Tokyo  
Kashiwanoha 5-1-5, Kashiwa, Chiba 277-8561, Japan  
arampath@gmail.com*

**Hajime Yamaguchi**

*Graduate School of Frontier Sciences, The University of Tokyo  
Kashiwanoha 5-1-5, Kashiwa, Chiba 277-8561, Japan  
h-yama@k.u-tokyo.ac.jp*

## Abstract

Recently, the Northern Sea Route (NSR) and Northwest Passage (NWP) have been opened to a greater extent due to sea-ice retreat in summer Arctic Ocean. This increases the possibility for the use of the NSR and NWP as a new Arctic sea route. Thus, a precise prediction system is vital for safe ship navigation in the NSR and NWP. To date, a lot of numerical studies have been carried out to forecast the overall Arctic sea ice for the climate change. With regards to the safe ship navigation, however, the accuracy and resolution in their model are still questionable. Our goal is to predict the ice edge up to 5 days ahead within an error of 10 km, using high-resolution (about 2.5 km) model. To date, an ice-ocean coupled model of the Arctic Ocean has been developed on the basis of the model. The atmospheric forcing components are given by the ERA-Interim with 6-hourly interval. After spinup of 10 years with the forcing data in 2000, the model was integrated from 2001 to 2013. The model reproduces the seasonal and interannual variations in the sea-ice extent and sea-ice drift velocity to some extent. However, the model showed relatively poor reproducibility on the simulation of the sea-ice thickness. As a first step toward the prediction of sea ice for the NSR and NWP, we conducted a series of hindcast and forecast simulations using the high-resolution model with simple data assimilation, and then compared with the satellite-induced sea ice.

*Proceedings of the 22nd IAHR International Symposium on Ice*

Copyright © 2014 IAHR 2014 Organizers. All rights reserved.

ISBN: 978-981-09-0750-1

doi:10.3850/978-981-09-0750-1\_1255

## **1. Introduction**

In September 2012, Arctic sea-ice extent reached the lowest minimum value ( $3.49 \times 10^6 \text{ km}^2$ ). The Northern Sea Route (NSR) and Northwest Passage (NWP) have been opened due to sea ice retreat in summer Arctic Ocean. The NSR and NWP are expected to be used as a commercial sea route, implying that the distances connecting Europe or North America and Asia are reduced by about 40% due to use of these routes. However, sea ice distribution varies from hour to hour with the weather and oceanic conditions. Thus, a precise prediction system of sea ice is vital for safe ship navigation in the NSR and NWP. In Japan, an Arctic Climate Change Research Project “Rapid Change of the Arctic Climate System and its Global Influences” have stated from 2011, under the Green Network of Excellence (GRENE) (<http://www.nipr.ac.jp/grene/e/index.html>) Program funded by the Ministry of Education, Culture, Sports, Science and Technology (MEXT). The GRENE program contains nine research projects in which studies on development of sea-ice prediction and ship navigation system are included. Yamaguchi (2013) describes the overview of the studies on sea-ice prediction, sea-ice monitoring, ship-ice interaction, ship icing, navigation scenario, and economic evaluation. As for sea-ice prediction, we have engaged in developing the system by two different approaches, which are short-term forecast of one-week timescale with numerical model and middle-term forecast of seasonal timescale with a statistical model using satellite data. Kimura et al. (2013) revealed an influence of winter sea-ice motion on summer ice cover in the Arctic using satellite data and furthermore created the statistical model for the NSR and NWP based on the results. In contrast, the short-term prediction system is indispensable for ships that navigate through the NSR and NWP. To date, we have developed an ice-ocean coupled model with middle-resolution (about 25 km) and high-resolutions (about 2.5 km) and have examined the sea-ice hindcast experiments (De Silva et al., 2014; Ono et al., 2014). The final goal of this study is to reproduce and predict the sea-ice edge up to 5 days ahead within errors of  $\pm 10 \text{ km}$  in regions of the NSR and NWP. In the current study, we investigated the model reproducibility and carried out a series of sea-ice forecasts, in addition to sea-ice hindcasts, to examine the predictability of sea-ice conditions.

## **2. Model description**

An ice-ocean coupled model of the Arctic Ocean (De Silva, 2013) has been developed on the basis of the model by Fujisaki et al. (2010). The ocean part is based on the Princeton Ocean Model (POM), a free surface, hydrostatic, primitive equation model (Blumberg and Mellor, 1987). The horizontal resolution is about 25 km for the whole Arctic Ocean (Fig. 1a) and about 2.5 km for the NSR (Fig. 1b) and NWP (Fig. 1c), and the vertical grid uses 33 sigma levels. The ice part consists of a dynamic model with the EVP rheology (Hunke and Dukowicz, 1997; Hunke, 2001) and 0-layer thermodynamic model (Semtner, 1979). In this model, sea ice is treated as ice bunch, which consists of floes aggregate and the semi-Lagrangian scheme, is also used. Ice bunch can be also arranged in the sub-grid scale. We also used the ice-collision rheology (Sagawa, 2007) for simulations in the NSR. The parameters used for the model are described in detail in De Silva (2013). The heat fluxes are calculated based on formulation of Parkinson and Washington (1979). Thickness change is solved by heat balance at upper and lower sea-ice surface. Albedo is 0.1 and 0.7 for ocean and sea ice, respectively. Snow effect is not considered in the current study. As the lateral boundary conditions, radiation and no-slip are

used for velocities and Pacific water inflow at Bering Strait is provided by the seasonal cycle of volume, temperature, and salinity. The atmospheric forcing components (air-temperature, dew-point temperature, wind, sea level pressure, and cloud) are given by the ERA-Interim with 6-hourly interval. After spinup of 10 years with the forcing data in 2000, the model was integrated from January 2001 to October 2013.

### 3. Model reproducibility

First, to investigate the reproducibility of a middle-resolution model, we compared the observed sea ice features with the simulated those. The model captured the magnitude and timing of the observed seasonal and interannual variations in the sea-ice area (Fig. 2a), which is defined as the cumulative sum of the area of the grid cells with at least 15% ice concentration multiplied by the ice fraction in the grid cell. As an example, simulated and observed ice concentrations for September 2007 are shown in Fig 2b and 2c, respectively. We found that the simulated spatial sea-ice concentration pattern as well as the location of the sea-ice edge (defined as 15% ice concentration contour) is nearly consistent with the Microwave Scanning Radiometer-Earth Observing System (AMSR-E) satellite data, except for some regions. Sea-ice draft from model is compared with draft measured by submarine, electromagnetic airborne measurements, drill holes, and upward looking sonars, which are available from the new Unified Sea Ice Thickness Climate Data Record (Lindsay, 2010). While the model underestimates the observed ice draft thicker than 2 m by 0.41 m (Fig. 3a), the correlation coefficient between them is relatively high (0.59). Sea-ice velocity from model is compared with buoy trajectories from International Arctic Buoy Program (IABP). In the Beaufort Sea (Fig. 3b) and regions off Laptev Sea, the simulated ice velocities give close agreement with the IAPB buoy data and the correlation coefficients between them are high and their biases are small.

### 4. Numerical simulations

As shown in Figs. 2 and 3, the middle-resolution model reproduced the observed sea-ice features to some degree. We here attempt to hindcast sea ice in a specified year with high-resolution models for the NSR. The models are driven by the ERA-Interim reanalysis data. The boundary and initial conditions are given by the results from the middle-resolution model. The target period for the NSR is 20 July to 31 December in 2004 and 2005. In the case of the NSR, the high-resolution model reproduced the time evolution in sea-ice extent well compared with the middle-resolution model, as shown in Figure 4. The simulated sea-ice extent with high-resolution model changes from  $1.8$  to  $1.5 \times 10^6 \text{ km}^2$  within four weeks, which is consistent with the observed result (red), but the simulated result with middle-resolution model (green) cannot reproduce such a reduction. This would be partly caused by effects of albedo and eddies as suggested by De Silva et al. (2014), which are remained as future works to reveal the detailed mechanism. The model also reproduced the opened date with the time lag of 4 days and the closed date with the time lag of 3 days, while the simulated sea-ice distribution is partly different from the observation and the closed place disagrees with the observation (not shown). Next, we performed a series of sea-ice hindcasts (not shown) and forecasts for the NWP in which the target period is 27 August to 1 September in 2013. In addition, to create more accurate sea-ice

states as an initial condition, we applied simple data assimilation (nudging) (e.g., Lindsay and Zhang, 2006) to the middle-resolution model using sea-ice concentration data from AVHRR, and then run the model from 30 December 2012 to 30 September 2013. As shown in Fig. 4, significant improvements can be seen in the ice concentration with data assimilation (red and green) compared with that without data assimilation (black). Correspondence of the assimilated and satellite-observed sea-ice area is generally quite good, except for the late June to middle August (Fig. 4). This is partly because we do not assimilate ocean parameters such as water temperature and salinity. In fact, the surface stratification structure was broken due to the sea-ice melting during this period (not shown). In the current study, since we focus on short-term sea-ice motion, we assume that ocean structures would not affect sea ice during the short-term period. However, we should reconsider data assimilation method in future. Using the assimilated sea-ice states on 27 August as an initial condition data, we conducted forecast of sea ice up to 5 days ahead with a high-resolution model. The atmospheric forecast data from ECMWF (ECM), Japan (JMA), Korea (KMA), UK (UKM), France (MFR), China (CMC), and Canada (CMA) are provided as forcing data. Figure 5 shows horizontal distributions in sea-ice concentration on 1 September from each forecast, in addition to the hindcast (ERA) using ERA-Interim data. There is no significant difference, but the distribution of sea-ice concentration with forcing from France appears to be slightly different from other results. However, even the hindcast with forcing from the ERA-Interim, the simulated sea-ice area underestimates the observed one, as shown in Figs 6a. In addition, the distances between the simulated and the satellite-observed sea-ice edge have large errors (Fig. 6b). These are partly because of the model bias.

## 5. Concluding remarks

We examined the model reproducibility and carried out a series of hindcast and forecast experiments, as the first step, to investigate the predictability of short-term sea-ice conditions for the NSR and NWP. Although the model captured observed sea-ice features to some degree, the simulated sea-ice edges have still errors. The current study partly includes the preliminary results. To improve the model forecast accuracy, the further studies would be necessary.

## Acknowledgments

This study was supported by Green Network of Excellence Program Arctic Climate Change Research Project.

## References

- Blumberg, A.F., and Mellor, G.L., 1987. A description of a three-dimensional coastal ocean circulation model. In: Heaps, N. (Eds.), *Three-Dimensional Coastal Ocean Models*, Coast. Estuar. Sci., vol. 4, AGU, Washington, DC, pp. 1–16.
- De Silva, L.W.A., 2013. Ice-ocean coupled computations for the sea ice prediction to support ice navigation in the Arctic Ocean, Dissertation, The University of Tokyo.

- De Silva, L.W.A., Yamaguchi, H., and Ono, J., 2014. A high-resolution hindcast study for the Northern Sea route. Proc. 29<sup>th</sup> International Symposium on Okhotsk Sea & Sea Ice.
- Fujisaki, A., Yamaguchi, H., and Mitsudera, H., 2010. Numerical experiments of air–ice drag coefficient and its impact on ice–ocean coupled system in the Sea of Okhotsk. Ocean Dyn., 60, 377–394, doi:10.1007/s10236-010-0265-7.
- Hunke, E.C., 2001. Viscous–Plastic Sea Ice Dynamics with the EVP Model: Linearization Issues. J. Comput. Phys., 170, 18–38, doi:10.1006/jcph.2001.6710.
- Hunke, E.C., and Dukowicz, J.K., 1997. An Elastic–Viscous–Plastic Model for Sea Ice, Dynamics. J. Phys. Oceanogr., 27, 1849–1867.
- Kimura, N., Nishimura, A., Tanaka, Y., and Yamaguchi, H. 2013. Influence of winter sea ice motion on summer ice cover in the Arctic, Polar Research, 32, 20193
- Lindsay, R.W., 2010. Unified Sea Ice Thickness Climate Data Record, Polar Science Center, Applied Physics Laboratory, University of Washington.
- Lindsay, R.W., and Zhang, J., 2006. Assimilation of ice concentration in an ice-ocean model, J. Atmos. Oceanic Technol., 23, 742-749.
- Ono, J., De Silva, L.W.A., and Yamaguchi, H., 2014. Modeling study of sea ice for the Northern Sea route: toward the short-term prediction. Proc. 29<sup>th</sup> International Symposium on Okhotsk Sea & Sea Ice.
- Parkinson, C.L., and Washington, W.M., 1979. A large-scale numerical model of sea ice. J. Geophys. Res., 84, 311–337, doi:10.1029/JC084iC01p00311.
- Sagawa, G., 2007. Development of ice dynamic model that takes account of floe collision and its validation in numerical sea ice forecast in the Sea of Okhotsk (in Japanese), Dissertation, The University of Tokyo.
- Semtner, A.J., 1976: A Model for the Thermodynamic Growth of Sea Ice in Numerical Investigations of Climate. J. Phys. Oceanogr., 6, 379–389.
- Yamaguchi, H., 2013. Sea ice prediction and construction of an ice navigation support system for the Arctic sea routes. Proc. 22<sup>nd</sup> International Conference on Port and Ocean Engineering under Arctic Conditions (POAC'13), ISBN 978-952-60-3635-9. ISSN 0376-6756, 8p.

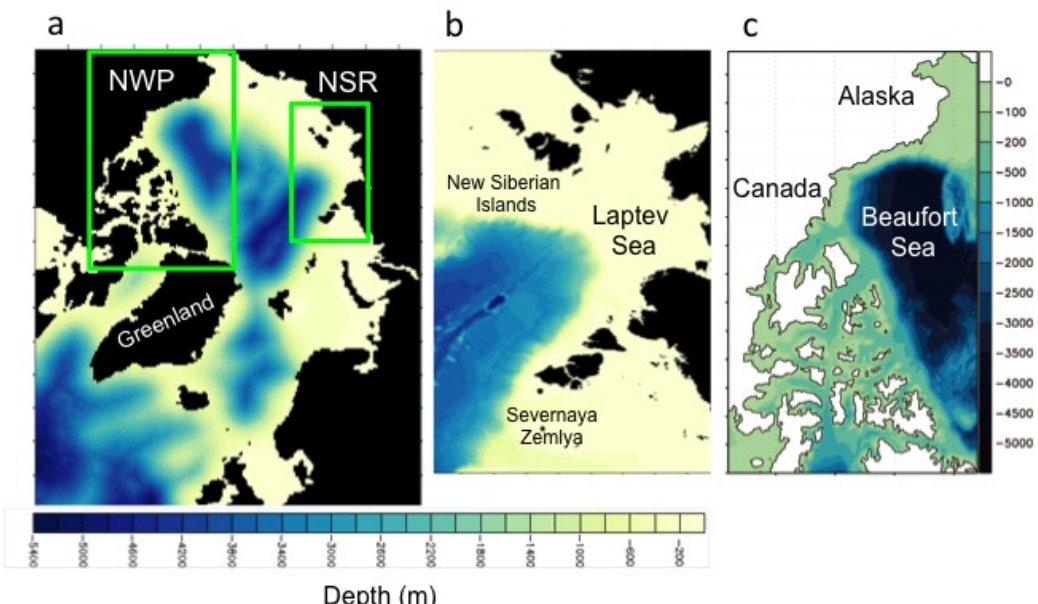


**Figure 1.** Model domain and bathymetry for (a) a whole Arctic model, (b) a regional model for NSR, and (c) a regional model for NWP. Bathymetry is derived from the ETOPO1 and the International Bathymetric Chart of the Arctic Ocean.

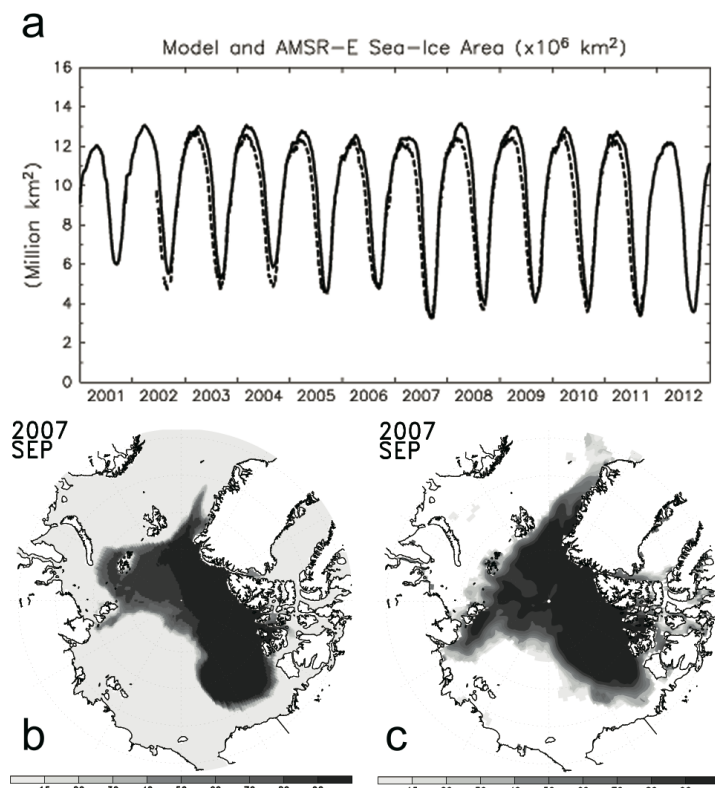


**Figure 2.** Daily time series of total sea-ice area from (a) the middle-resolution model (solid line) and AMSR-E (dashed line). Distribution of monthly averaged sea-ice concentration in September from (b) the middle-resolution model and (c) AMSR-E.

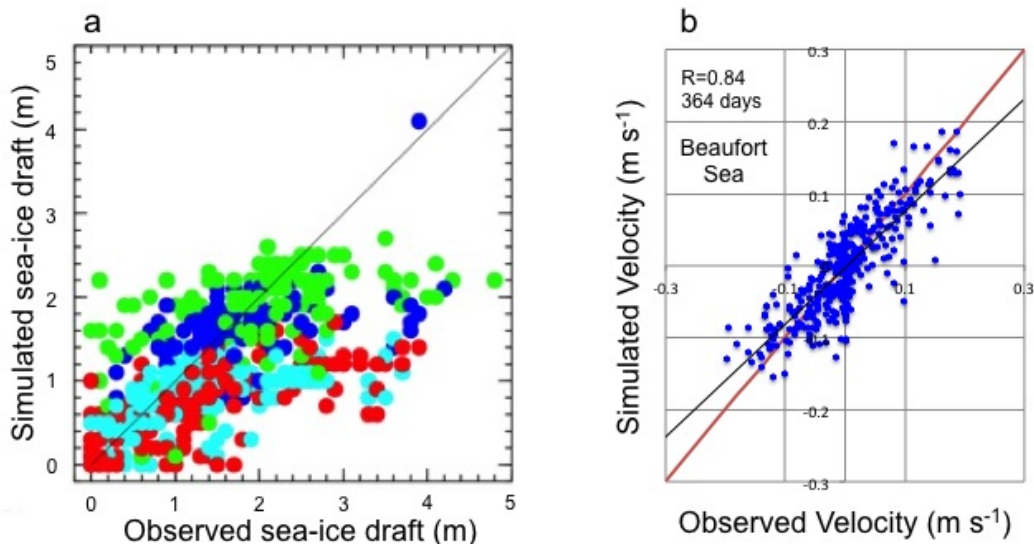


**Figure 3.** (a) Simulated and observed sea-ice draft (Lindsay, 2010) and (b) Simulated and Observed sea-ice velocity from IABP.

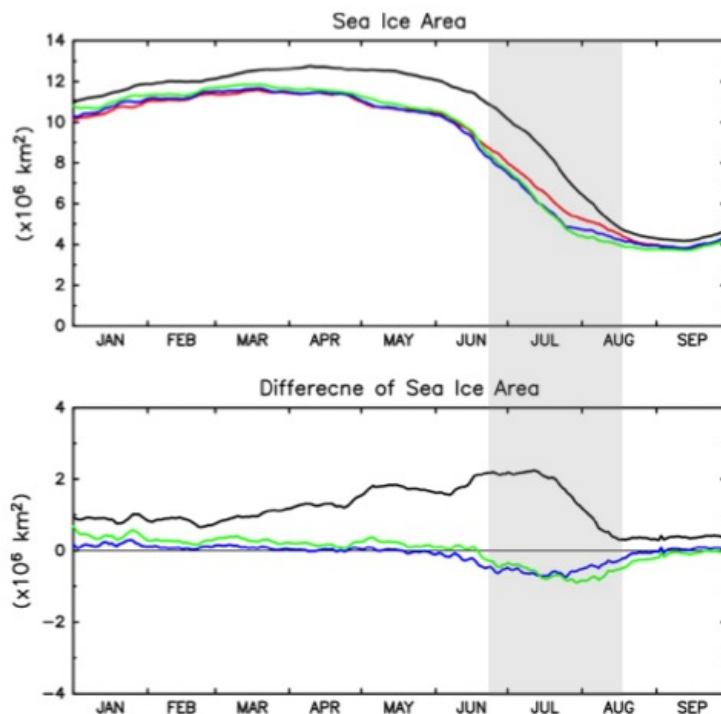


**Figure 4.** (Upper) Time series of sea ice area from the satellite observation (AVHRR, red), the middle-resolution model with data assimilation with 1 days (blue) and 5 days (green) restored time, and without data assimilation (black). (Lower) Time series of difference in sea ice area between model and satellite observation.

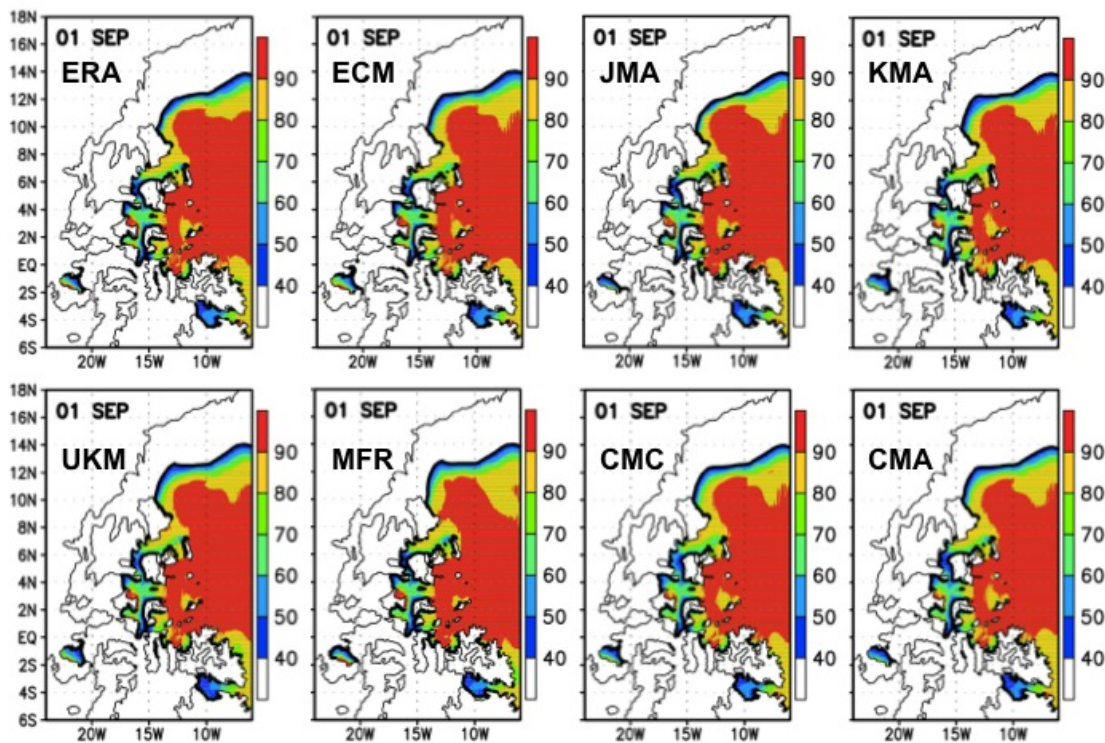


**Figure 5.** Horizontal distributions in sea-ice concentration on 1 September 2013, using atmospheric forcing data from ERA-Interim (ERA), data. CMWF (ECM), Japan (JMA), Korea (KMA), UK (UKM), France (MFR), China (CMC), and Canada (CMA).

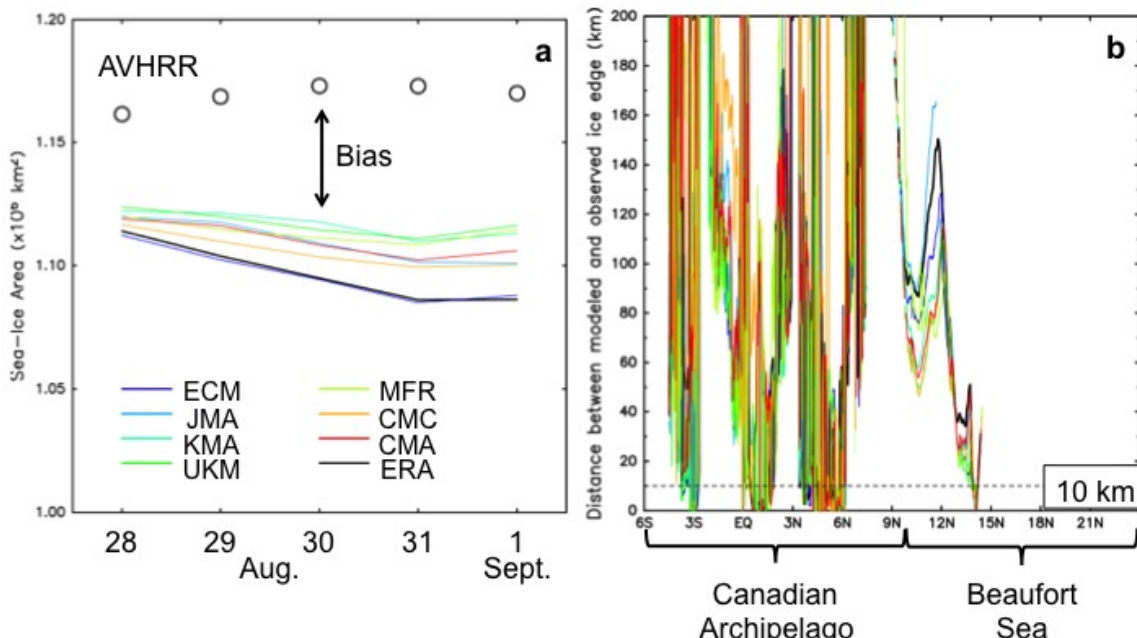


**Figure 6** (a) Sea-ice area in August 28 to September 1, 2013, and (b) distance between modeled and observed sea-ice edge, in each simulations. In (b), the horizontal axis indicates the latitude in the model coordinate, as shown in Fig. 5.